Algerian Journal of Environmental Science and Technology
March edition. Vol.7. Nº1. (2021)
ISSN : 2437-1114
www.aljest.org

Rigorous modeling and simulation of the reactive absorption of CO_2 with loaded aqueous monoethanolamine solution

I. Hammouche, A. Selatnia*, R. Derriche

Fossil Energy Valorization Laboratory, Chemical Engineering Department, National Polytechnic School, 10 Avenue Hassen Badi, BP 182, El Harrach, Algiers, Algeria.

*Corresponding author: ammarselatnia@yahoo.fr; Tel.: +213 6 56 06 09 37; Fax: +21300 00 00

ARTICLE INFO

Article History:

Received : ***21/11/2018***
Accepted : ***28/11/2019***

***Key Words*:**

Carbon dioxide removal;
Absorption–desorption;
Post-combustion;
Packed absorber column;
Rate-based model.

ABSTRACT/RESUME

Abstract: *In recent years, significant efforts have been made to mitigate greenhouse gas emissions from industrial sources and prevent the worldwide climate change. Special attention has been given to carbon dioxide removal using absorption–desorption with chemical solvents. A reliable design, scale up, control, and optimization of post-combustion CO_2 capture processes requires the use of an accurate packed bed absorber modeling and simulation. In this paper, a rigorous rate-based model that describes the reactive absorption of carbon dioxide into loaded aqueous monoethanolamine solution in a countercurrent-flow packed absorber column has been developed. The model considers both mass and heat fluxes across the interface; thus, liquid and gas phases are balanced separately. Proper correlations currently available in literature for physico-chemical as well as heat and mass transfer properties estimation were included into the model to ensure reliable predictions; all equations (mass and energy balances, equilibrium speciation, kinetic model, enhancement factor model as well as the physico-chemical and transport properties) were then implemented in MATLAB software. The developed model was successfully validated against published experimental data with maximum average relative deviation percentages less than 2.8 % and 1.7 % for liquid temperature and CO_2 loading profiles, respectively.*

I. Introduction

Carbon dioxide emissions from industrial sources have become a serious environmental issue seen their great impact on the global warming which is estimated to be more than 60% compared to other greenhouse gases as stated by Moulijn et al. [1]. Its concentration in the atmosphere is approximately 400ppm, upper about 300ppm from the pre-industrial level[2]. This high CO_2 atmospheric concentration alters the energy balance of the earth's climate system that rises the planet's global average temperature of about 0.74 °C since 1906 until 2005 as reported by Core-Writing-Team [3].

In the recent years, the world is concerned by the growth and the developmen of various methods and technologies for CO_2 removal from gas streams. In regards to this area, Post-combustion capture by chemical absorption using aqueous solutions of alkanolamines is the most mature and promising technology [4-5]. furthermore, it has been proved as one of the less expensive methods to be applied to power plants as confirmed by Erga et al., [6].

The most commonly used, suitable, mature and well-documented chemical solvent for acid gas absorption is aqueous solutions of monoethanolamine due to its high reaction rate, relatively low cost, and its thermal stability.

Furthermore, it is often considered as a base case solvent in many research works [7-10]

The current study focuses on the development of a rigorous rate-based model to simulate the reactive absorption of CO2 with loaded aqueous MEA solution to ensure a reliable design, scale up, control, and optimization of post-combustion CO_2 capture processes. The model takes into account the mass transfer resistances in the liquid and gas films as well as the heat effects associated with the reactive absorption through material and energy balances in both gas and liquid phases. The most suitable and recent correlations and methods for the calculation of physicochemical as well as mass and heat transfer properties are incorporated into the model to guarantee accurate predictions.

The rate-based model was then validated by simulating a number of experiments on the absorption of CO_2 in monoethanolamine solutions carried out in packed-bed absorbers. In this context, the experimental data reported in literature by Sonderby et al. [11] was selected as the basis for this simulation study; where they used a pilot absorber column with a total height of 10.5m and an internal diameter of 0.1 m. It is made of pyrex glass and packed with Sulzer Mellapak 250Y. The column consists of 10 sections each 1.0m high. Redistributors are located between sections. The packing height for each section is 0.82m and thus a maximum effective absorption height of 8.2m can be obtained and the packing diameter is 0.084 m.

II. Rate-based model

Three types of the rate-based model have been applied for the modeling and simulation of packed columns for CO_2 absorption: the continuous differential contactor model (CDC), the continuous film reaction model, and non equilibrium stage model. In this study, the CDC model has been used; this model was first proposed by Pandya [12] based on the differential-change approach suggested by Treybal [13] and was largely employed by many authors; however, it has been found that it presents some inconsistent simplifications or assumptions; therefore, Llano-Restrepo and Araujo-Lopez [14] revised the model using the finite difference approach and introduced a new improved version.

II.1. Material and energy balances in the gas and liquid phases

In this paper, the improved version of the CDC model suggested by Llano-Restrepo and Araujo-Lopez [14] is applied, which consists of a set of five ordinary differential equations describing mass and energy balances in a packed column.

- A steady state mole balances on CO_2 and water vapor

$$\frac{dY_A}{dz} = \frac{-k_{G.A}\, a\, P(y_A - y_{A.I})}{G_B} \tag{1}$$

$$\frac{dY_S}{dz} = \frac{-k_{G.S}\, a\, P(y_S - y_{S.I})}{G_B} \tag{2}$$

- A steady-state total mole balance for both liquid and gas phases

$$\frac{dL}{dz} = G_B\left(\frac{dY_A}{dz} + \frac{dY_S}{dz}\right) \tag{3}$$

- Temperature gradients for the gas and liquid phases

$$\frac{dT_G}{dz} = \frac{-h_G(T_G - T_L)\, a}{G_B(C_{p.B}^{(g)} + Y_A C_{p.A}^{(g)} + Y_S C_{p.S}^{(g)}} \tag{4}$$

$$\begin{aligned}\frac{dT_L}{dz} = \frac{G_B}{LC_{P,L}}\Bigg\{&\left[C_{p.B}^{(g)} + Y_A C_{p.A}^{(g)} + Y_S C_{p.S}^{(g)}\right]\frac{dT_G}{dz} \\ &+ \left[C_{p.A}^{(g)}(T_G - T_0) - \Delta H_{rx}^{(abs)}(T_0) - C_{P,L}(T_L - T_0)\right]\frac{dY_A}{dz} \\ &+ \left[C_{p.S}^{(g)}(T_G - T_0) - \Delta H_{vap,S}(T_0) - C_{P,L}(T_L - T_0)\right]\frac{dY_S}{dz}\Bigg\}\end{aligned} \tag{5}$$

II.2. Equilibrium speciation model

The equilibrium speciation model developed by Matin et al. [15] was used in this study in order to determine the liquid-bulk chemical species concentrations required for all calculations. The model was founded on the following reactions occurred when CO_2 reacts with loaded aqueous MEA solution.

- Ionization of water:

$$2H_2O \leftrightarrow OH^- + H_3O^+ \tag{6}$$

- Dissociation of dissolved CO_2 through carbonic acid:

$$CO_2 + 2H_2O \leftrightarrow HCO_3^- + H_3O^+ \tag{7}$$

- Dissociation of bicarbonate:

$$HCO_3^- + H_2O \leftrightarrow CO_3^{2-} + H_3O^+ \tag{8}$$

- Carbamate reversion to bicarbonate (hydrolysis reaction):

$$RNHCOO^- + H_2O \leftrightarrow RNH_2 + HCO_3^- \tag{9}$$

- Dissociation of protonated amine:

$$RNH_3^+ + H_2O \leftrightarrow RNH_2 + H_3O^+ \tag{10}$$

Noting that R stands for C_2H_4OH.

According to the above reactions, the chemical spices concentrations in question are $OH^-, H_3O^+, HCO_3^-, CO_2, CO_3^{2-}$, RNH_3^+, RNH_2 , and $RNHCOO^-$. In this context, Matin et al. [15] solved a set of eight non-linear algebraic equations (including the chemical reaction equilibriums as well as the material and charge balances) by means of the Newton-Raphson method to obtain a valid

Algerian Journal of Environmental Science and Technology
March edition. Vol.7. Nº1. (2021)
ISSN : 2437-1114
www.aljest.org

simplified form of the speciation model. Consequently, the resulting equilibrium concentrations are related through the following expressions:

$$[RNH_2] = (1 - 2\alpha_A)[RNH_2]_0 \quad (11)$$
$$[RNHCOO^-] = \alpha_A[RNH_2]_0 \quad (12)$$
$$[RNH_3^+] = \alpha_A[RNH_2]_0 \quad (13)$$

Where $[RNH_2]$ and $[RNH_2]_0$ are the free and the total MEA concentrations, respectively.

II.3. Kinetic model

An extensive number of experimental and theoretical studies have been reported in literature on the kinetics of carbon dioxide reacting with unloaded aqueous MEA solution since 1950's. However, only few researchers have studied the kinetics of carbon dioxide absorption into partially carbonated MEA solutions [16-21]. The most recent model for the second-order rate constant, the one developed by Luo et al. [21], have been used in this study, this kinetic model is based on the termolecular mechanism, and expressed as follow:

$$k_2 = k_{2,MEA}[MEA] + k_{2,H_2O}[H_2O] \quad (14)$$
$$k_{2,MEA} = 2.003 * 10^{10} \exp\left(\frac{-4742}{T_L}\right) \quad (15)$$
$$k_{2,H_2O} = 4.147 * 10^6 \exp\left(\frac{-3110}{T_L}\right) \quad (16)$$

The kinetic model is valid over temperature, MEA concentration and CO_2 loading ranges of (298-343) K, (1 and 5) M, and (0-0.4) $mol_{CO2}/\ mol_{MEA}$, respectively.

II.4. Enhancement Factor model

The mass transfer of CO_2 in the liquid phase is enhanced by the chemical absorption relative to the physical one. Thus, the enhancement factor is expressed as follow:

$$E = \frac{k_{L.A}}{k^0_{L.A}} \quad (17)$$

For (m+n)th order reversible reaction, Gaspar and Fosbøl [22] introduced a new implicit model for the enhancement factor calculation; this model was validated with the two-film model numerical solution, and represented by the following set of equations:

$$E_i = 1 + \left(\frac{C_R D_R}{\nu D_{A,L} C_{A,I}}\right) \quad (18)$$
$$(1 - E_i)Y^2 + Ha(y_{A.I} - 1)Y + E_i - y_A = 0 \quad (19)$$
$$Y = \sqrt{y_R^i} \quad (20)$$
$$E = Ha\sqrt{y_R^i}\,\frac{1 - y_{A.I}}{1 - y_A} \quad (21)$$

II.5. Interfacial compositions

The CO_2 and water mole fractions $y_{A.I}$ and $y_{S.I}$, respectively, at the gas-phase side of the interface are given below:

$$y_{A.I}\,P = \frac{y_A\,P + \left(\frac{Ek^0_{L.A}}{k_{G.A}}\right)C_A}{1 + \frac{1}{He}\left(\frac{Ek^0_{L.A}}{k_{G.A}}\right)} \quad (22)$$

$$y_{S.I} = x_S\,\gamma_S\,P_S^{sat}/P \quad (23)$$

Indicating that the model considers the liquid phase as an ideal solution, thus $\gamma_S = 1$ and Raoult's law $y_{S.I} = x_S\,P_S^{sat}/P$ is valid.

II.6. Physicochemical and transport properties

All correlations and methods for physico-chemical and transport properties calculation used in the current study were presented in **Table 1.** Indicating that the selection of liquid-phase properties was based on a comparative analysis of different correlations available in literature with experimental data where the most suitable ones (that fit better experimental data) were determined for each property.

III. Simulation of the rate-based model

In order to solve the differential equations which describe mass and energy balances included in the rate-based model applied to the reactive absorption of CO_2 in packed-bed absorber, a computer program was coded in Matlab software. Figure 1 provides a simplified flowchart that explain breifly the program algorithm.

Table 1 . *List of correlations used in the current study for the estimation of physico-chemical and transport properties*

Liquid phase properties			
Property	**correlation**	**Property**	**correlation**
Density of pure MEA	Jayarathna et al. [23]	Diffusivity of N_2O in water	Jamal [27]
Density of water	Kell [24]	Diffusivity of N_2O in aqueous MEA solution	Ko et al. [29]
Density of CO_2-loaded MEA solution	Weiland et al. [25]	Diffusivity of MEA in water	Snijder et al. [30]
Viscosity of water	Swindells taken from Weast [26]	Surface Tension of CO_2-loaded aqueous MEA solution	Jayarathna et al. [23]
Viscosity of CO_2-loaded MEA solution	Weiland et al. [25]	Heat capacity of liquid MEA	Agbonghae et al. [31]
Henry's constant of CO_2 in water	Jamal [27]	Heat capacity of liquid water	Agbonghae et al. [31]
Henry's constant of N_2O in water	Jamal [27]	Heat capacity of CO_2-loaded aqueous MEA solution	Agbonghae et al. [31]
Henry's constant of N_2O in aqueous MEA solution	Jiru et al. [28]	Heat of absorption of CO_2 in aqueous MEA solution	Llano-Restrepo and Araujo-Lopez [14] based on Arcis et al. [32] data
Diffusivity of CO_2 in water	Jamal [27]	Heat of vaporization	Pitzer et al. [33]
Gas phase properties			
Property	**correlation**	**Property**	**correlation**
Gas phase density	Soave [34] Holderbaum and Gmehling [35]	Gas phase CO_2 diffusivity	Wilke [40]
Gas phase viscosity	Poling et al. [36]	Thermal conductivity of pure gases	Ely and Hanley method taken from Reid et al. [41]
Gas phase heat capacities	Smith et al. [37]	Gas phase thermal conductivity	Wassiljewa–Mason–Saxen method taken from Poling et al. [36]
Gas phase binary diffusivities	Fuller method taken from Poling et al. [36]	Gas phase water vapor diffusivity	Blanc' s expression taken from Poling et al. [36]
Water vapor pressure	Antoine [38]		
Mass and heat transfer properties			
Property	**correlation**	**Property**	**correlation**
Mass transfer coefficients	Billet and Schultes [42]	Gas phase heat transfer coefficient	Geankoplis [43]
Effective interfacial area	Billet and Schultes [42]	mass-transfer-corrected gas-phase heat transfer coefficient	Pandya [12]
Liquid holdup of packing	Billet and Schultes [42]		

Algerian Journal of Environmental Science and Technology
March edition. Vol.7. Nº1. (2021)
ISSN : 2437-1114
www.aljest.org

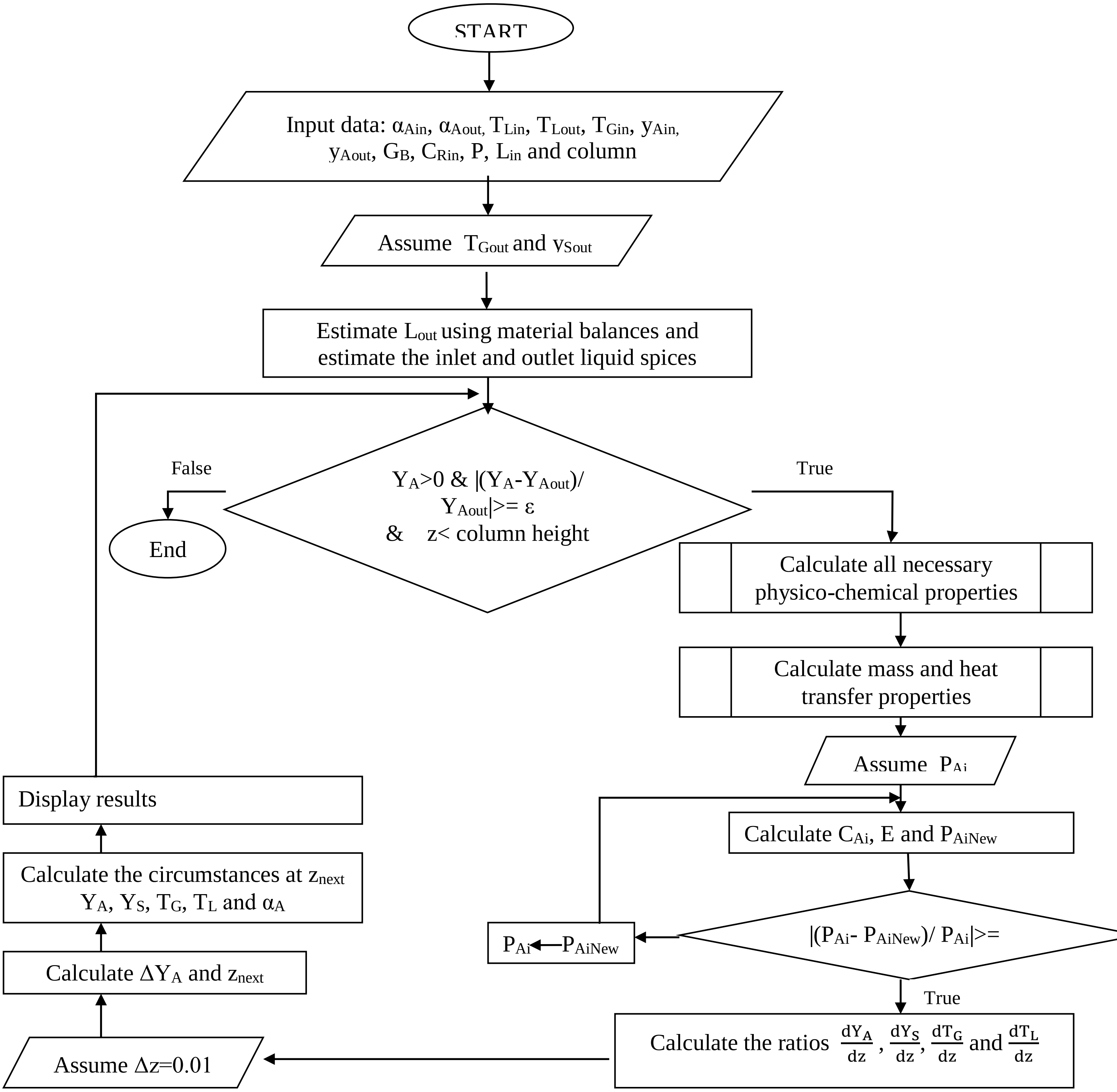

Figure1. *Flowchart for the rate-based model simulation*

IV. Results and discussion

In this section, the simulation results obtained while modeling and simulating the reactive absorption of CO_2 with loaded aqueous MEA solution were validated against pilot-plant experimental data reported by Sonderby et al. [11]. The results are presented in term of liquid and gas temperature, liquid CO_2 loading as well as carbon dioxide and water vapor gas phase mole fraction profiles along the packed column height.

In this paper, the average relative deviation percentage ARD% was used to compare model predictions with experimental data, and it was calculated by means of the following equation:

$$\mathrm{ARD\%} = 100 * \frac{1}{n}\sum_{1}^{n}\left(\frac{x_i^{cal} - x_i^{Exp}}{x_i^{Exp}}\right) \qquad (24)$$

where x_i^{Exp} and x_i^{cal} are the experimental and calculated process parameters of component i, respectively.

IV.1. Temperature profiles

The predicted temperature profile obtained while using the rate-based model is very significant due to the fact that it depends on many model parameters, for instance, heat of absorption, CO_2 solubility in amine solutions, kinetic model, heat and mass properties, and other physicochemical properties.
The packed-bed absorber modeled in this study operates in counter-current mode. The lean solvent and the rich CO_2 flue gas are fed from to the top and the bottom of the column, respectively. The liquid temperature coming down from the top is increased due to the heat released under the effect of the reactive absorption of CO_2 in the amine solution; In the other hand, the flue gas coming up from the bottom received a part of the evolved heat of the rich solvent and rise the flue gas temperature from the column bottom upwards to the near top. Furthermore, the heat of reaction causes the vaporization of water which is then condensed due to the colder solvent coming from the top of the column. Hence, a significant temperature bulge, as shown in Figures 2 and 3, can be observed in the temperature profiles of the absorber. Indicating that the temperature bulge location and magnitude are affected by many parameters such as, the liquid-gas ratio, the point where CO_2 is absorbed into the amine solution, and the heat of reaction [44].

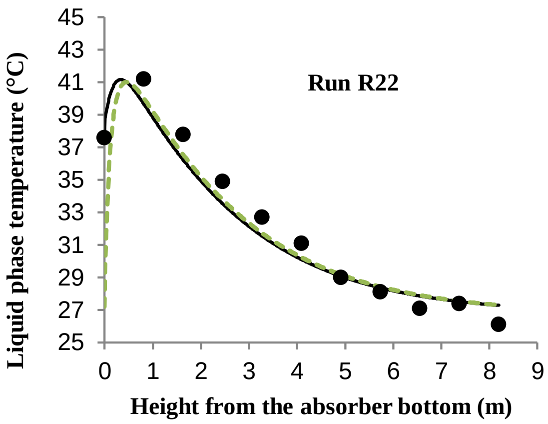

Figure2. *Profiles of Liquid and gas phase temperatures along the absorber height for run R22. Filled circles: experimental data; solid and dotted curved lines: simulation results for the liquid and gas phase temperatures, respectively.*

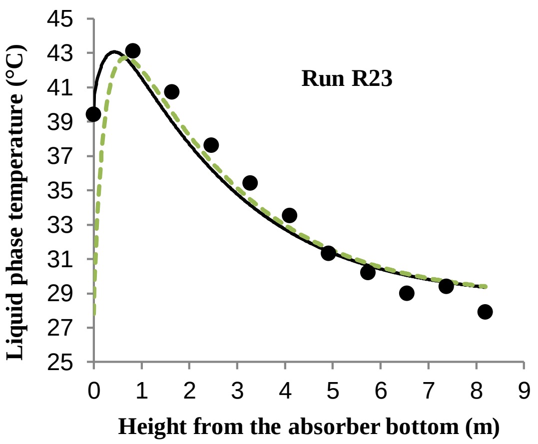

Figure3. *Profiles of Liquid and gas phase temperatures along the absorber height for run R23. Filled circles: experimental data; solid and dotted curved lines: simulation results for the liquid and gas phase temperatures, respectively.*

Figures 2 and 3 show the predicted liquid and gas phase temperatures along the absorber height compared to the liquid phase experimental profiles for runs R22 and R23 of Sonderby et al. [11]. According to these figures, It has been observed that near the bottom the liquid phase temperature exceeds the gas phase temperature; however, along the most of the column is the inverse which means that the gas-phase temperature exceeds slightly the liquid-phase temperature. It has been also noticed that an overall agreement between measured and predicted liquid temperatures is generally good for both runs (R22 and R23) with an average relative deviation percentage ARD% of 2.76 and 2.79, respectively. However, the liquid temperature is somewhat overpredicted in the last 2m of the absorber for both runs, that could be explained by the use of empirical correlations to estimate the

Algerian Journal of Environmental Science and Technology
March edition. Vol.7. Nº1. (2021)
ISSN : 2437-1114
www.aljest.org

different model parameters affecting the temperature profiles (kinetic model, transport properties, heat of absorption, and physicochemical properties); hence, a judicious selection of these parameters is very essential to guarantee reliable predictions.

IV.2. Liquid CO_2 loading profiles

One of the key design parameter of an absorber column is the liquid CO_2 loading (mole of CO_2 per mole of MEA).

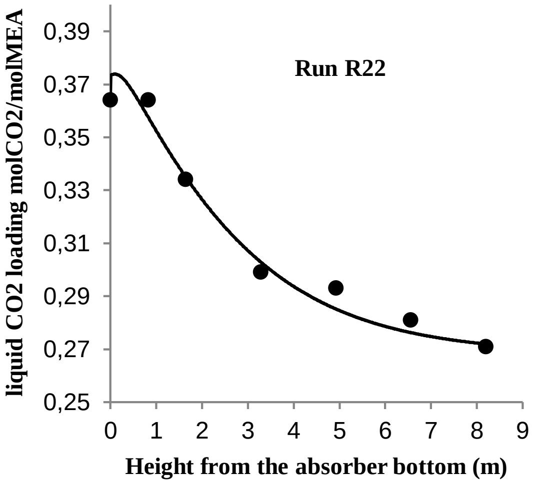

Figure4. *Profiles of Liquid CO_2 loading mol_{CO2}/mol_{MEA} along the absorber height for run R22. Filled circles: experimental data; solid lines: simulation results.*

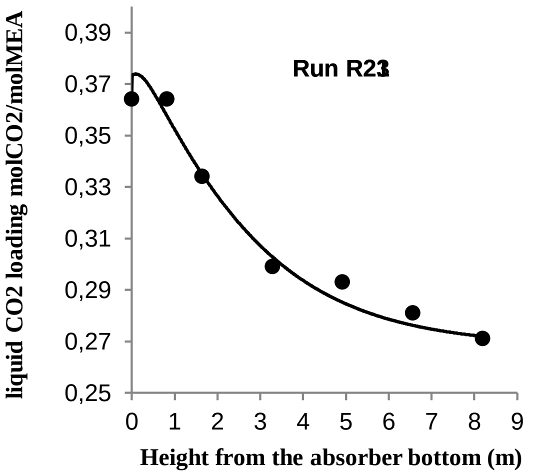

Figure5. *Profiles of Liquid CO_2 loading mol_{CO2}/mol_{MEA} along the absorber height for run R23. Filled circles: experimental data; solid lines: simulation results.*

In regards to this area, the predicted liquid CO_2 loading profiles compared with the corresponding experimental profiles obtained from runs R22 and R23 of Sonderby et al. [11] are illustrated in Figures 4 and 5. Based on these Figures, it is clear that the predicted and measured CO_2 loading profiles are almost coinciding for both runs (R22 and R23) with a very low average relative deviation percentage ARD% of about 1.15 and 1.69, respectively.

IV.3. Carbone dioxide and water vapor profiles

Figures 6 and 7 illustrate simulation results for the carbon dioxide and water vapor mole fraction profiles in the gas phase compared with the measured carbon dioxide mole fractions along the absorber height obtained from runs R22 and R23 of Sonderby et al. [11]. Accordingly, it has been noticed that the agreement between experimental data and simulation predictions is generally good in both cases or runs. However, the predicted outlet CO_2 concentration in the gas phase is slightly underpredicted in R22 and overpredicted in R23. Moreover, the CO_2 mole fraction in the gas phase decreases rapidly in the bottom part of the column, which indicate that most CO_2 removal takes place in this region; the remaining height of the absorber serves to further reduce the carbon dioxide concentration to reach a very small value for the exiting gas stream; whereas, the water vapor mole fraction in the gas phase increases near the bottom region of the absorber under the effect of the evaporation from the liquid phase then it decreases until reaching an asymptotic value under the effect of gas phase condensation.

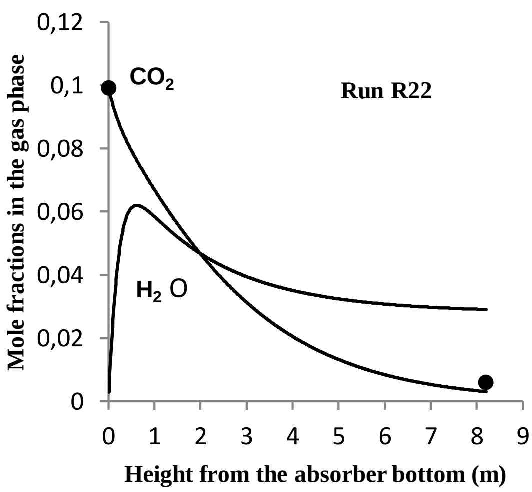

Figure6. *Profiles of the carbon dioxide and water vapor gas phase mole fractions along the absorber height for run R22. Filled circles:*

experimental data; solid curved lines: simulation results.

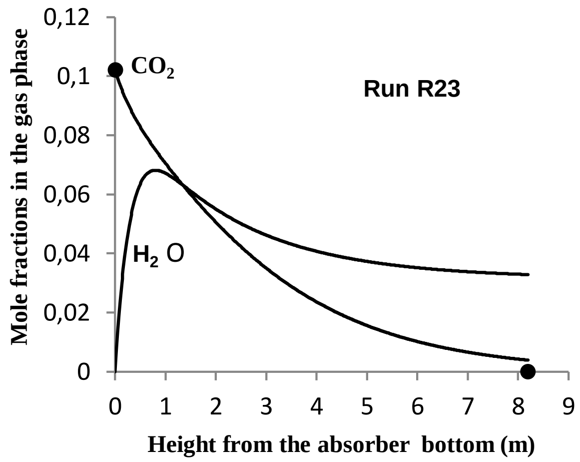

Figure7. *Profiles of the carbon dioxide and water vapor gas phase mole fractions along the absorber height for run R23. Filled circles: experimental data; solid curved lines: simulation results.*

V. Conclusion

In this study, a rigorous rate-based model that describes the reactive absorption of CO_2 with a loaded aqueous MEA solution in a packed-bed absorber was developed. The model was then implemented in Matlab software in order to solve the differential equations (mass and energy balances).The simulation results obtained were then validated against a number of experimental measurements reported in the open literature. The comparison between predicted and experimental profiles for liquid temperature and CO_2 gas mole fraction presents an excellent agreement with very low average relative deviation percentages less than 2.8 % and 1.7 %, respectively.

VI. Nomenclature

a	mass-transfer interfacial area per packing unit volume, m^2/m^3
C_A	molar concentration of free CO_2 in the liquid phase, mol/ m^3
$C_{p,G}$	gas-phase molar isobaric heat capacity, J/(mol K)
$C_{P,L}$	liquid-phase molar isobaric heat capacity, J/(mol K)
$C_{p.i}^{(g)}$	gas-phase molar isobaric heat capacity of species i, J/(mol K)
$D_{A,L}$	liquid-phase diffusivity of CO_2, , m^2/s
D_R	The liquid-phase diffusivity, m^2/s
E	enhancement factor
G_B	molar flow rate of carrier gas B per unit cross section area, mol/(s m^2)
Ha	Hatta number
He	Henry's law constant,
h_G	gas-phase convective heat transfer coefficient, J/(s K m^2)
k_2	second-order reaction rate constant, m^3/(kmol s)
$k_{G.i}$	gas side mass-transfer coefficient of component i, kmol/(kPa m^2 s)
$k_{L.A}^0$	the ordinary liquid-phase mass transfer coefficient, m/s
L	liquid-phase molar flow rate per unit cross section area, mol/(s m^2)
P	gas-phase total pressure, Pa
P_S^{sat}	vapor pressure of species S, Pa
T_0	reference temperature (298.15K)
T_G	gas-phase temperature, K
T_L	liquid-phase temperature, K
x_S	mole fraction of water vapor in the liquid bulk
Y_i	gas-phase mole ratio of species i (with respect to carrier gas B)
y_i	mole fraction of species i in bulk gas phase
$y_{i.I}$	mole fraction of species i in gas-phase side of interface
z	column height, m
Greek symbols	
α_A	CO_2 loading, mole CO_2/mole MEA
$\Delta H_{rx}^{(abs)}$	molar heat of reactive absorption of CO_2, kJ/mol of CO_2
$\Delta H_{vap,S}$	molar heat of vaporization of water, J/mol
ν	stoichiometric coefficient
Subscripts	
A	carbon dioxide
ARD%	average relative deviation percentage
B	carrier gas
MEA	monoethanolamine
R	MEA
S	water vapor

VII. Refrences

1. Moulijn, J. A.; Stankiewicz, A.; Grievink, J.; Górak. Process intensification and process systems engineering: a friendly symbiosis. *Computers & Chemical Engineering* 32 (2008) 3-11.
2. Oh, T. H. Carbon capture and storage potential in coal-fired plant in Malaysia. *Renewable and Sustainable Energy Reviews* 14 (2010) 2697-2709.
3. Core-Writing-Team. Climate Change 2007 Synthesis Report (No. AR4). *Inter governmental Panel on Climate Change, Geneva, Switzerland* (2007).
4. Mofarahi, M.; Khojasteh, Y.; Khaledi, H.; Farahnak, A. Design of CO_2 absorption plant for recovery of CO_2 from flue gases of gas turbine. *Energy* 33 (2008) 1311-1319.
5. MacDowell, N.; Florin, N.; Buchard, A.; Hallett, J.; Galindo, A.; Jackson, G.; Adjiman, C.; Williams, C.; Shah, N.; Fennell, P. An overview of CO_2 capture technologies. *Energy & Environmental Science* 3(2010) 1645-1669.
6. Erga, O.; Juliussenb, O.; Lidal, H. CO_2 recovery by means of aqueous amines. *Energy Conversion and Management* 36 (1995) 387-392.
7. Mohammadpour, A.; Mirzaei, M.; Azimi, A. Dimensionless numbers for solubility and mass transfer rate of CO_2 absorption in MEA in presence of additives. *Chemical Engineering Research & Design* (2019). https://doi.org/10.1016/j.cherd.2019.06.026.
8. Ali Saleh Bairq, Z.; Gao, H.; Huang, Y.; Zhang, H.; Liang, Z. Enhancing CO_2 desorption performance in rich MEA solution by addition of SO42−/ZrO2/SiO2 bifunctional catalyst. *Applied Energy* 252 (2019) 1-1.
9. Akinola, T. E.; Oko, E.; Wang, M. Study of CO_2 removal in natural gas process using mixture of ionic liquid and MEA through process simulation. *Fuel* 236 (2019) 135-146.

10. Wang, J.; Deng, S.; Sun, T.; Xu, Y.; Li, K.; Zhao, J. Thermodynamic and cycle model for MEA-based chemical CO_2 absorption. *Energy Procedia* 158 (2019) 4941-4946.
11. Sonderby, T.L.; Carlsen, K.B.; Fosbol, P.L.; Kiorboe, L.G.; von Solms, N. A new pilot absorber for CO_2 capture from flue gases: measuring and modelling capture with MEA solution. *International Journal of Greenhousse Gas Control* 12 (2013) 181-192.
12. Pandya, J.D. Adiabatic gas absorption and stripping with chemical reaction in packed towers. *Chemical Engineering Communications* 19 (1983) 343-361.
13. Treybal, R.E. Adiabatic gas absorption and stripping in packed towers. *Industrial & Engineering Chemistry* 61(1969) 36-41.
14. Llano-Restrepo, M.; and Araujo-Lopez, E. Modeling and simulation of packed-bed absorbers for post-combustion capture of carbon dioxide by reactive absorption in aqueous monoethanolamine solutions. *International Journal of Greenhousse Gas Control* 42 (2015) 258-287.
15. Matin, N.S.; Remias, J.E.; Neathery, J.K.; Liu, K.. Facile method for determination of amine speciation in CO_2 capture solutions. *Industrial & engineering chemistry research* 51(2012) 6613-6618.
16. Littel, R. J.; Versteeg, G. F.; Van Swaaij, W. P. M. Kinetics of CO_2 with primary and secondary amines in aqueous solutions-II. Influence of temperature on zwitterion formation and deprotonation rates. *Chemical Engineering Science* 47(1992) 2037-2045.
17. Aboudheir, A.; Tontiwachwuthikul, P.; Chakma, A.; Idem, R. Kinetics of the reactive absorption of carbon dioxide in high CO_2-loaded concentrated aqueous monoethanolamine solutions. *Chemical Engineering Science* 58(2003) 5195-5210.
18. Dang, H.; Rochelle, G. T. CO_2 Absorption Rate and Solubility in Monoethanolamine/ Piperazine/Water. *Separation & Science Technology* 38(2003) 337-357.
19. Puxty, G.; Rowland, R.; Attalla, M. Comparison of the rate of CO_2 absorption into aqueous ammonia and monoethanolamine. *Chemical Engineering Science* 65(2010) 915-922.
20. Dugas, R. E.; Rochelle, G. T. CO_2 absorption rate into concentrated aqueous monoethanolamine and piperazine. *Journal of Chemical Engineering Data* 56(2011) 2187-2195.
21. Luo, X.; Hartono, A.; Hussain, S.; Svendsen, H.F. Mass transfer and kinetics of carbon dioxide absorption into loaded aqueous monoethanolamine solutions. *Chemical Engineering Science* 123(2015) 57-69.
22. Gaspar, J. ; Fosbøl, P.L. A general enhancement factor model for absorption and desorption systems: A CO_2 capture case-study. *Chemical Engineering Science* 138 (2015) 203-215.
23 Jayarathna, S.A.; Weerasooriya, A.; Dayarathna, S.; Eimer, D.A.; Melaaen, M.C. Densities and surface tensions of CO2 loaded aqueous monoethanolamine solutions with r = (0.2 to 0.7) at T = (303.15 to 333.15) K. *Journal of Chemical Engineering Data* 58(2013) 986-992.
24. Kell, G. S. Density, Thermal Expansivity, and Compressibility of Liquid Water from 0 to 150 °C: Correlations and Tables for Atmospheric Pressure and Saturation reviewed and Expressed on 1968 Temperature Scale. *Journal of Chemical Engineering Data* 20(1975) 97-105.
25. Weiland, R. H.; Dingman, J. C.; Cronin, D. B.; Browning, G. J. Density and Viscosity of Some Partially Carbonated Aqueous Alkanolamine Solutions and Their Blends. *Journal of Chemical Engineering Data* 43(1998) 378-382.
26. Weast, R. C. Handbook of Chemistry and Physics, 65th edition. *CRC* 1984
27. Jamal, A. Absorption and desorption of CO_2 and CO in alkanolamine systems. *Ph.D, Thesis, University of British Columbia, Canada* 2002.
28. Jiru, Y.; Eimer, D.A.; Wenjuan, Y. Measurements and correlation of physical solubility of carbon dioxide in (monoethanolamine + water) by a modified technique. *Industrial & engineering chemistry research* 51 (2012) 6958-6966.
29. Ko, J. J.; Tsai, T. C.; Lin, C. Y. Diffusivity of Nitrous Oxide in Aqueous Alkanolamine Solutions. *Journal of Chemical Engineering Data* 46(2001) 160-165.
30. Snijder, E.D.; te Riele, M.J.M.; Versteeg, G.F.; Van Swaaij, W.P.M. Diffusion coefficients of several aqueous alkanolamine solutions. *Journal of Chemical Engineering Data* 38(1993) 475-480.
31. Agbonghae, E.O.; Hughes, K.J.; Ingham, D.B.; Ma, L.; Pourkashanian, M. A semi-empirical model for estimating the heat capacity of aqueous solutions of alkanolamines for CO_2 capture. *Industrial & engineering chemistry research* 53(2014) 8291-8301.
32. Arcis, H.; Ballerat-Busserolles, K.; Rodier, L.; Coxam, J.-Y. Enthalpy of solution of carbon dioxide in aqueous solutions of monoethanolamine at temperatures of 322.5 K and 372.9 K and pressures up to 5 MPa. *Journal of Chemical Engineering Data* 56 (2011) 3351-3362.
33. Pitzer, K. S.; Curl, R. F. The Thermodynamic Properties of Fluids. *Inst. Mech. Eng., London* 1957.
34. Soave, G. Equilibrium constants from a modified Redlich-Kwong equation of state. *Chemical Engineering Science* 27 (1972) 1197-1203.
35. Holderbaum, T.; Gmehling, J. PSRK: a group contribution equation of state based on UNIFAC. *Fluid Phase Equilibia* 70 (1991) 251-265.
36. Poling, B.E.; Prausnitz, J.M.; O'Connell, J.P. The Properties of Gases and Liquids. *McGraw-Hill, New York* 2001.
37. Smith, J.M.; van Ness, H.C.; Abbott, M.M. Introduction to Chemical Engineering Thermodynamics, 7th edition. *McGraw-Hill, New York* 2005.
38. Antoine, C. Tensions of the vapors; new relationship between the voltages and temperatures. *Meeting Reports of the Academy of Sciences* 107 (1888) 681-684.
39. Wilke, C.R. Diffusional properties of multicomponent gases. *Chemical Engineering Progress* 46 (1950) 95-104.
40. Reid, R.C.; Prausntiz, J.M.; Poling, B.E. The Properties of Gases and Liquids. *Mc-Graw Hill, New York* 1987.
41. Billet, R.; Schultes, M. Prediction of mass transfer columns with dumped and arranged packings. *Chemical Engineering Research and Design* 77(1999) 498-504.
42. Geankoplis, C.J. Transport Processes and Separation Process Principles, 4th edition. *Prentice-Hall* 2003.
43. Kvamsdal, H.; Rochelle, G. Effects of the temperature bulge in CO_2 absorption from flue gas by aqueous monoethanolamine. *Industrial & Engineering Chemistry Research* 47(2008) 867-875.

Please cite this Article as:
Hammouche I., Selatnia A., Derriche R., Rigorous modeling and simulation of the reactive absorption of CO2 with loaded aqueous monoethanolamine solution ***Algerian J. Env. Sc. Technology**, **7**:**1 **(2021) 1777-1786**